KADUNA JOURNAL OF GEOGRAPHY
2026, VOL. 8, No. 1, 827-846
https://doi.org/10.47514/kjg.2026.08.01.077

Research Article

Climate Variability, Urbanisation, and Cereal Crop Yield in Gwagwalada Area Council, Federal Capital Territory, Abuja, Nigeria: A 31-Year Assessment

Stephanie Anastasia Obodo [a], Isaiah Majin Sule [a], Ishiaku Ibrahim [a]

[a] Department of Geography, Federal University of Technology, Minna, Nigeria.

ABSTRACT

This study examines cereal-yield trends and the socio-ecological relationships among urbanisation, climate variability, and staple-crop productivity in Gwagwalada Area Council, Federal Capital Territory, Abuja, Nigeria (1994-2024), with scenario-based projections to 2050. Focusing on maize, millet, and rice, the study integrated multi-temporal Landsat land-use/land-cover (LULC) classification (1994, 2004, 2024), climate-trend analysis, crop- yield assessment (2010-2022 verified records; 1994-2009 and 2023-2024 extrapolated), relationship testing, variance partitioning, and Cellular Automata-Markov (CA-Markov) simulation. Between 1994 and 2024, built-up area expanded by 245.68% (58.82 to 203.33 km²), while farmland declined by 48.12% (536.04 to 278.11 km²). Annual mean temperature increased significantly by 0.037˚C/year (~1.14˚C total), whereas rainfall exhibited a non- significant decline. Despite farmland contraction, maize, millet, and rice yields increased by 136.55%, 180.68%, and 44.44%, respectively. Across the three LULC milestones (n=3), urbanisation showed perfect positive co-movement with crop yields (rs = 1.00; R^2 = 0.960-0.995), reflecting structural alignment rather than causal proof. Over the 31- year series, rainfall and temperature jointly explained 19.59% (maize), 13.96% (millet), and 25.23% (rice) of yield variance. A verified-data robustness check (n = 13) showed temperature remained dominant for maize and millet while rainfall became principal for rice, with substantial unexplained variance (54.12%-76.99%) indicating strong non-climatic influences. By 2050, CA-Markov projections indicate built-up area will reach 351.72 km² (+72.98%) while farmland falls to 212.34 km² (−23.65%). Under 40% maize, 35% millet, and 25% rice allocations, scenario- based production increases by 21.6% (511,372 MT), 26.8% (465,364 MT), and 0.5% (270,147 MT), respectively, supporting farmland-protection zoning within FCT Master Plan revisions.

ARTICLE HISTORY
Submitted 10 September 2026
Accepted 30 October 2026
Published 27 November 2026

GUEST EDITOR
A. M. Ahmed

KEYWORDS
Urbanisation; crop yield; climate variability; CA-Markov simulation; peri-urban agriculture; FCT Abuja; land-use change; food production.

1 Introduction

Climate variability remains one of the most pressing challenges of our time, with its effects rippling across ecological, agricultural, and socioeconomic systems, driving global malnutrition by diminishing diet diversity and overall food consumption due to droughts, marking its critical role in climate change (Franzke et al., 2020). The fluctuations in weather conditions over time create substantial difficulties in ensuring a stable supply of food, reducing poverty, and promoting development in affected regions (Muhammad et al., 2021).

Global empirical evidence shows that urban expansion over the past 25 years has reduced cropland and net primary productivity by 58.71 TgC, equivalent to roughly 14.4 million tons of grain, enough to meet the minimum annual grain intake of approximately 36 million people (Huang et al., 2020). Government policies such as the Land Use Act and the Abuja Master Plan have created path dependencies that are generating persistent challenges for current governance efforts (Ibe et al., 2023). Migration from the Abuja Municipal Area Council to more affordable councils like Gwagwalada has accelerated population growth, contributing to a decline in green areas, increased vehicular traffic, reduced farmland, and lower living standards (Cobbinah, 2023). Spatial assessments across the FCT confirm that rapid urban sprawl is steadily consuming surrounding agricultural and vegetated zones, driven by high urban development pressure along Abuja's expanding corridors (Aniekwe & Igu, 2022; Igbokwe et al., 2024).

Enoguanbhor et al. (2021) documented land-use planning governance challenges in the Abuja city-region but did not examine crop yield outcomes. Ibilewa et al. (2021) assessed cropland exposure to climate variability in the FCT but did not integrate urbanisation trends or future projections. Amaechi and Hassan (2022) analysed climate risk in the FCT but did not link findings to crop productivity. Rowland and Ebuka (2024) examined LULC change and urban infrastructure but excluded agricultural yield as an outcome variable. Similarly, Mshelia et al. (2024) modelled land-cover transitions and vegetation dynamics in Abuja but did not link these spatial shifts to staple cereal productivity. Taken together, these studies have examined urbanisation, climate variability, and environmental change in and around

Corresponding Author: Obodo, S, A. obodosmte407@st.futminna.edu.ng Department of Geography, Federal University of Technology, Minna, Nigeria
© 2026 The Author(s)

Gwagwalada and the FCT, but none has simultaneously quantified crop yield trends, urbanisation–yield relationships, and spatially explicit 2050 production projections within one integrated analytical framework. This study addresses that gap by integrating land cover change analysis, climate trend analysis, crop yield trends, relationship testing, and CA-Markov simulation into one framework. In doing so, it offers a local evidence base for planning, agricultural protection, and climate adaptation in one of the fastest-growing peri-urban territories in the FCT.

The contribution to knowledge is threefold: it links land use change to crop outcomes in a peri-urban FCT setting, tests whether climate or non-climate factors better explain cereal yield patterns, and provides a practical basis for projecting agricultural outcomes alongside urban expansion. The present study explicitly frames this as a localised, spatially explicit, and longitudinal study intended to inform sustainable land use planning and food policy.

The overall aim of the study is to assess how climate variability and urbanisation have influenced cereal crop yield in Gwagwalada Area Council from 1994 to 2024 and to project the likely implications of continued urban growth to 2050, using these specific objectives:

i. Examine crop yield trends for maize, millet, and rice from 1994-2024
ii. Examine the relationship between climate variables, urbanisation, and crop yield
iii. Simulate the impact of urbanisation on crop production by 2050.

2 Literature Review

2.1 Climate Variability and Crop Yield

Climate variability refers to the inherent tendency of the climate of a specific area to fluctuate over time, encompassing shifts in temperature, precipitation, humidity, and other meteorological elements across seasonal, interannual, and multi-decadal timescales (Franzke et al., 2020). In practical terms, the realised temperature and precipitation in any given year can deviate markedly from the long-term climatology; some years are warmer or colder than normal, and some wetter or drier, driven in part by large-scale ocean–atmosphere oscillations such as El Niño, which shifts irregularly every two to seven years and causes short-term spikes or dips in global temperatures (Bonan, 2015).

Yiran et al. (2020) observed that many cities across sub-Saharan Africa, including Nigeria, are expanding at an annual rate of 3.6 percent and mounting pressure on infrastructure that directly undermines the agricultural systems surrounding rapidly expanding urban cores. Low productivity across the continent is linked to the limited availability and accessibility of agricultural inputs, lack of access to climate-resilient technologies and machinery, and the instability of weather conditions that characterise sub-Saharan African farming environments (Serote et al., 2023).

Ankrah et al. (2023) examined climate variability adaptation strategies and their effect on maize yield in the Cape Coast Municipality of Ghana, finding that farmers who adopted deliberate adaptation strategies achieved significantly better yield outcomes than those who did not, underscoring the importance of institutional support and extension services in enabling effective smallholder adaptation. Mubenga-Tshitaka et al. (2023) examined climate variability impacts on agricultural output in East Africa, finding that rainfall variability and temperature anomalies exert statistically significant negative effects on agricultural output across the region, with smallholder farmers particularly vulnerable given their overwhelming dependence on rainfed agriculture.

Rapid population growth, projected urbanisation rates, and socioeconomic transformations continue to pressure Nigeria's limited arable land and agricultural productivity (Wudil et al., 2023). Urban sprawl, propelled by both natural population growth and rural-to-urban migration, is progressively encroaching on fertile farmlands, narrowing the space for food production and complicating the country's agricultural landscape (Wudil et al., 2023; Okeleye et al., 2023). These studies collectively indicate that the relationship between rainfall, temperature, and crop yield is context-specific, modified by intensification, market access, and management adaptation conditions that are increasingly present in the peri-urban setting of Gwagwalada, and that the present study explicitly tests against empirical data.

2.2 Urbanisation and Agricultural Land Use in Sub-Saharan Africa

Urbanisation is a complex process that involves the increase in the proportion of urban population over time (Deppisch & Yilmaz, 2021). It also involves aggregation of people into large, dense settlements and has both positive and negative impacts on society and the environment (Wang et al., 2020). The world's population continues to grow rapidly, with global estimates projecting roughly 9.7 billion people by 2050 who will all require access to sufficient, nutritious food (United Nations Department of Economic and Social Affairs [UN DESA], 2024). Africa remains the fastest-growing region globally, projected to increase its share of the world's population from 19% to 26% by 2050 and drive unprecedented urban expansion (UN DESA, 2024).

Recent studies across Nigeria and comparable analyses have consistently found that urban expansion has significantly reduced agricultural land. The land-use analysis of Niger, Kwara, and Benue states (1990–2020)

revealed that decades of population growth and migration led to substantial conversion of cropland and natural vegetation into built-up areas, placing pressure on both farmland and ecosystem services (Okeleye et al., 2023). The impact on local food production and markets shows that reclamation of farmland for built infrastructure has notable repercussions for local food systems. This is evident in a study of Niger, Kwara, and Benue, which shows that as agricultural land diminished, crop yields fluctuated, exacerbated by youth migration and abandonment of fields, thus undermining food availability (Okeleye et al., 2023).

Peri-urban agriculture has become increasingly important within urban food systems, especially in low- and middle-income nations. It plays a crucial role in improving food crop production by delivering fresh agricultural products to city markets and providing economic opportunities for residents in peri-urban zones. Haysom and Battersby (2023) highlight that this form of agriculture enhances urban food system resilience through its adaptability and decentralized nature, making it capable of withstanding disruptions caused by climate variability and market instability. Collectively, the literature demonstrates that urban expansion can reduce agricultural land while also creating conditions for peri-urban intensification and improved market access. The outcome therefore depends on whether productivity gains from intensification can offset the longer-term loss and fragmentation of farmland, an issue examined in the Gwagwalada case.

2.3 CA-Markov Modelling and Peri-Urban Simulation

The CA-Markov model combines the probabilistic temporal projection capabilities of the Markov Chain with the spatially explicit simulation capabilities of Cellular Automata, producing land use change projections that are both temporally realistic and spatially meaningful (Sang et al., 2011). Tahir et al. (2025) applied CA-Markov modelling and GIS techniques to predict land use and land cover changes for sustainable land management, demonstrating the model's capacity to generate reliable future land use scenarios across diverse environmental and governance contexts. Mansour et al. (2020) monitored land use and land cover changes in the mountainous cities of Oman using GIS and CA-Markov modelling techniques, finding that the model effectively captured the spatial pattern and direction of urban expansion and agricultural land loss even in topographically complex environments, confirming the model's adaptability across diverse landscape contexts.

Enoguanbhor et al. (2022) simulated urban land expansion in the context of land use planning in the Abuja city-region using CA-Markov, finding that urban expansion follows a clear centrifugal pattern outward from Abuja's core into surrounding satellite towns, including Gwagwalada, with agricultural land bearing the heaviest burden of conversion under business-as-usual growth trajectories. Imhanfidon et al. (2023) conducted a geospatial assessment of physical expansion in urban development in Bwari Area Council, a neighbouring area council to Gwagwalada in the FCT, finding that urban land expansion has dramatically reduced vegetated and agricultural land cover over the study period, providing localised empirical precedent for the land use change dynamics this study documents in Gwagwalada. These applications demonstrate the usefulness of CA-Markov modelling for identifying likely spatial patterns of urban expansion and agricultural-land conversion. The present study extends this approach by connecting the projected LULC changes to crop-specific yield and production outcomes under a 2050 scenario.

3 Materials and Methods

3.1 Study Area

Gwagwalada Area Council lies between Latitudes 8° 53′ 0″ and 9° 30′ 0″ N of the Equator and Longitudes 6° 51′ 30″ and 7° 17′ 0″ E of the Greenwich Meridian. It is one of the six area councils of the Federal Capital Territory (FCT), Abuja, covering an official administrative landmass of approximately 1,069 km², and is bounded by Bwari and Abuja Municipal Area Council (AMAC) to the north and east, Kwali Area Council to the south, and Abaji Area Council to the west. However, for the purpose of this spatial analysis and mapping layout, the digital administrative boundary utilized encompasses a total classified surface area of 911.99 km² (Figure 1).

The region features a tropical continental climate with distinct wet and dry seasons. The rainy season starts between March and April and ends between September and October, while the dry season begins in November. Published background estimates suggest a typical annual rainfall range of approximately 1,120–1,500 mm (Chunwate et al., 2021); however, the CHIRPS record used in this study (1994–2024) shows that early years of the series experienced anomalously high rainfall, with 1994 and 1995 recording 1,922.9 mm and 1,937.4 mm respectively, before the record stabilised closer to the climatological norm in subsequent decades. Ambient temperatures typically range from a mean minimum of 26 °C around December and January to a mean maximum of 35 °C during the peak of the dry season in March and April.

Socio-economically, the inhabitants are mostly farmers, practicing both rain-fed and irrigation farming. To supplement household income, they also engage in secondary non-agricultural activities such as woodcutting, poultry farming, and blacksmithing. Additionally, the area hosts a population of civil servants

who work in various ministries, commercial industries, and academic institutions as their primary or secondary occupations (Aina & Sule, 2025).

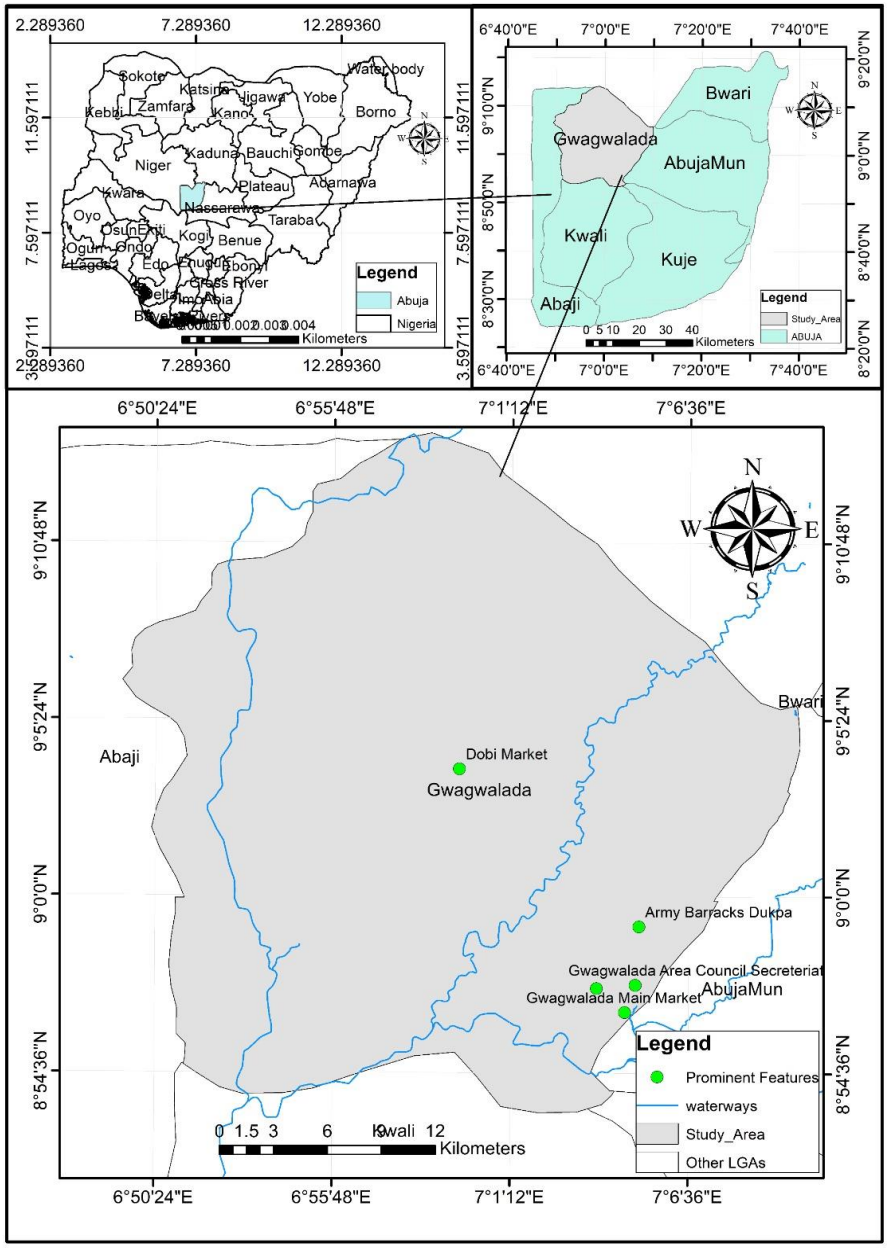

Figure 1: The Study Area

3.2 Data Sources

Crop yield data were obtained from the Agricultural Development Project, with original records covering 2010–2022 and missing years for 1994–2009 and 2023–2024 extrapolated for trend analysis. The study focused on three cereal crops: maize, millet, and rice, because they are widely grown and are useful indicators of crop yield change in the council. Crop yield was measured in metric tonnes per hectare (MT/ha), while cultivated area was measured in hectares (ha). The present study also defines the extrapolated values separately from the original records, which is important for transparency in the trend analysis. Land use and land cover data were derived from three classified Landsat epochs: 1994, 2004, and 2024. These images were classified into built-up area, farmland, vegetation, bare surface, and water bodies using supervised classification in a GIS environment. Climate data consisted of annual rainfall (mm) and annual mean temperature (°C), from 1994–2024, sourced from CHIRPS. These data were used to examine climate variability and its relationship with crop yield over the same period.

3.3 Crop Trend Analysis

Crop yield trend analysis was carried out using descriptive statistics to summarise the level and variability of maize, millet, and rice yields over time. The thesis specifies mean yield, standard deviation, coefficient of variation, overall percentage change, year-on-year change, minimum yield, and maximum yield as the main

statistics.

3.4 Relationship Analysis

The climate-yield relationship was assessed using Pearson correlation, with annual rainfall and temperature paired against each crop yield series across 31 annual observations. Pearson's (r) was appropriate because both climate variables and crop yield were treated as continuous variables over the same time span.

Urbanisation relationships were analysed using Spearman rank correlation because built-up area data were available for only three epochs: 1994, 2004, and 2024. The thesis applies this non-parametric method to evaluate the directional alignment of urbanisation with crop yield and local temperature over time. For urbanisation-linked comparisons across epochs, percentage change and descriptive trend comparisons were also used. To maintain methodological rigor and prevent the introduction of compounded statistical errors, the study deliberately avoided calculating annual interpolated built-up area values. A portion of the continuous annual crop yield timeline relies on extrapolated estimates; pairing them with interpolated spatial metrics would risk generating an unverified statistical relationship. To formalise the descriptive magnitude and linear fit of these structural changes, a simple linear regression model ($\hat{Y} = a + bX$) was executed strictly across the three classified land use and land cover milestones. Crucially, because only three aligned observations were available ($n = 3$), resulting in one residual degree of freedom ($df_{residual} = 1$), this regression framework was applied as a descriptive tool to estimate linear trend trajectories and co-movements. Parametric significance testing and statistically interpretable p-values were deliberately omitted as they are invalid at this sample size, and the model was not used to establish explicit causal mechanisms (Conover, 1999) and was formulated as Equation (1):

$$\hat{Y} = a + bx \quad (1)$$

Where Ŷ represents the predicted continuous dependent variable, corresponding either to the localized cereal crop yield (expressed in metric tonnes per hectare, MT/ha, for maize, millet, or rice) or the annual mean temperature (°C). The term a denotes the unobservable baseline model intercept constant, while b represents the descriptive slope coefficient that quantifies the absolute rate of change per unit increase in the physical built-up area. The independent variable X denotes the absolute surface extent of the physically classified built-up area footprint (expressed in square kilometers, km²).

The five-class urbanisation framework (Class 1: very low-density rural; Class 2: low-density peri-urban; Class 3: medium-density transitional urban; Class 4: high-density urban; Class 5: very high-density urban core) was applied to classify urbanisation extent across the study period. This classification is adapted from established urban density typologies used in global human settlement research, particularly the Global Human Settlement Layer (GHSL) framework developed by the European Commission's Joint Research Centre (Kemper et al., 2016; Melchiorri et al., 2018), and the multi-class urban intensity framework applied by Schneider and Woodcock (2008) across twenty-five global cities. Alongside the regression's slope coefficient (b) and coefficient of determination (R^2), the thesis derives a yield-per-urbanisation rate (r_u), which expresses the absolute change in crop yield per unit increase in built-up area. This descriptive rate coefficient is later used directly in the 2050 crop projection formula, serving as an operational bridge between historical trend analysis and future spatial simulation.

Concurrently, the longitudinal climate-yield dynamics and the localized variance partitioning were evaluated across the continuous 31-year empirical observation timeline (1994–2024, n = 31). To isolate the localized predictive strength of fluctuating meteorological elements from broader peri-urban socio-ecological drivers, a multi-variable parametric ordinary least squares (OLS) regression framework was deployed as Equation (2):

$$Y = \beta_0 + \beta_1(RF) + \beta_2(Temp) + \varepsilon \quad (2)$$

Where Y represents the continuous observed annual cereal crop yield series over the 31-year timeline (MT/ha), β_0 denotes the structural intercept configuration of the OLS model, and β_1 and β_2 represent the partial regression slope coefficients assigned to the localized rainfall and environmental temperature parameters, respectively. The term RF defines the continuous annual rainfall observation series (expressed in millimeters, mm), $Temp$ indicates the continuous annual mean temperature observation series (°C), and ε represents the stochastic residual error term capturing all non-climatic variance components, structural market transformations, and peri-urban input intensification factors.

3.5 2050 Simulation

Spatiotemporal projections targeting the 2050 milestone were operationalized using a hybrid Cellular Automata-Markov Chain (CA-Markov) modeling architecture. This dual-stage methodology links the non-spatial stochastic temporal probabilities derived from historical transition trends with a spatially explicit local neighborhood allocation filter. The temporal quantity component is governed by the standard Markovian framework, expressed as Equation (3):

$$S(t + 1) = P_ij \times S(t) \quad (3)$$

Where $S(t)$ represents the discrete multi-class land use and land cover state matrix verified at the initial base epoch (t = 2024), and $S(t + 1)$ denotes the simulated land use and land cover configuration matrix projected for the target destination epoch (t + 1 = 2050). The operational operator P_ij defines the calculated transition probability matrix, which captures the temporal likelihood that a spatial cell belonging to LULC class i will transition into LULC class j over the discrete operational time steps.

To establish spatial dependency and resolve the physical location of projected land cover changes, the Cellular Automata spatial allocation filter acts upon the temporal output. The geographic distribution of simulated cell state changes is modeled as a function of neighboring localized spatial contiguity rules, formulated as Equation (4):

$$S(t + 1) = f\,(\,S(t), N\,) \tag{4}$$

Where S represents the finite set of discrete thematic geographic states distributed across the cellular lattice space, N denotes the physical dimensions and weighting values of the localized neighborhood filter configuration matrix (e.g., standard pixel configuration rules), and f represents the local transition rule function that dictates cellular state changes based on neighboring thematic proximity and pre-defined multi-criteria evaluation suitability inputs.

To avoid applying the full projected farmland area independently to every crop, the 2050 agricultural area was allocated among the three crops using assumed shares based on the proportional distribution implied by the verified 2010–2022 ADP cropping pattern. Maize was assigned 40%, millet 35%, and rice 25% of the projected 2050 farmland area. Thus, of the projected 212.34 km² of farmland, approximately 84.94 km² was allocated to maize, 74.32 km² to millet, and 53.08 km² to rice, equivalent to 8,494 ha, 7,432 ha, and 5,308 ha, respectively. For comparability, the same crop-specific shares were applied to the 2024 farmland baseline when estimating revised 2024 production. This ensures that the percentage changes between 2024 and 2050 reflect the projected scenario rather than a change in allocation assumptions. Finally, to evaluate the downstream consequences of physical urban expansion on long-term agricultural food security, a descriptive two-stage crop production scaling projection framework was constructed. Stage 1 projects the expected per-hectare cereal yield by leveraging the derived historical yield-per-urbanisation sensitivity coefficient (ru) against the simulated built-up expansion, as in Equation (5):

$$Y\,2050 = Y\,2024 + ru \times (Bu\,2050 - Bu\,2024) \tag{5}$$

Where $Y\ 2050$ represents the projected per-hectare crop yield for the target year 2050 (MT/ha), $Y\ 2024$ denotes the empirical baseline crop yield observed during the 2024 milestone (MT/ha), and ru represents the derived historical yield-per-urbanisation rate coefficient, measuring absolute yield change per unit increase in built-up area (MT/ha per km²). The terms $BU\ 2050$ and $BU\ 2024$ correspond to the simulated 2050 and classified 2024 physical built-up area (km²), respectively. Stage 2 scales the projected per-hectare yield directly against the net available agricultural surface area simulated by the CA-Markov engine to output the aggregate regional yield mass. The production calculation is presented in Equation (6):

$$TP\ 2050c = Y2050c \times FA2050c \tag{6}$$

Where c denotes the crop, and $FA\ 2050c$ is the crop-specific farmland allocation. This approach avoids the methodological error of assuming that the entire projected farmland base is simultaneously planted with each crop. This structure is important because it links land expansion directly to expected yield change and then scales that result by projected farmland area. The study notes that the projection should be interpreted as a scenario based on continuation of historical relationships, not as a fixed forecast under all possible future policy or technology conditions.

4 Results

4.1 Crop Yield Trends, 1994–2024

Table 1 presents the descriptive statistics for maize, millet, and rice yields over the 1994–2024 period. Maize recorded a mean yield of 26.12 MT/ha, an overall percentage change of +136.55 percent, and a coefficient of variation of 35.79 percent, indicating moderate interannual variability.

Table 1: Summary Descriptive Statistics of Crop Yield (1994-2024)

Statistic	Maize	Millet	Rice
Mean Yield (MT/ha)	26.12	21.30	30.62
Standard deviation	9.35	9.54	3.97
Minimum yield (MT/ha)	15.98	10.66	21.70
Maximum yield (MT/ha)	42.60	37.14	38.68
Coefficient of variation (%)	35.8	44.8	13.0
Overall percent Change (1994-2024)	+136.5	+180.7	+44.4

Millet had the lowest mean yield among the three crops at 21.30 MT/ha but the highest overall percentage change at +180.68 percent and the highest CV at 44.80 percent, showing that it was the most variable crop over time. Rice recorded the highest mean yield at 30.62 MT/ha, the lowest CV at 12.98 percent, and an overall percentage change of +44.44 percent, making it the most stable crop in the series.

Figure 2 shows the three yield trend lines from 1994 to 2024, with maize and millet appearing more volatile than rice. Across the three crops, a common pattern emerges during the extrapolated periods (1994–2010): gradual, proportional yield growth broadly aligned with farm size expansion. The divergence in behaviour becomes apparent in the original data phase (2010–2022), where crop-specific responses to continued farm expansion differ markedly.

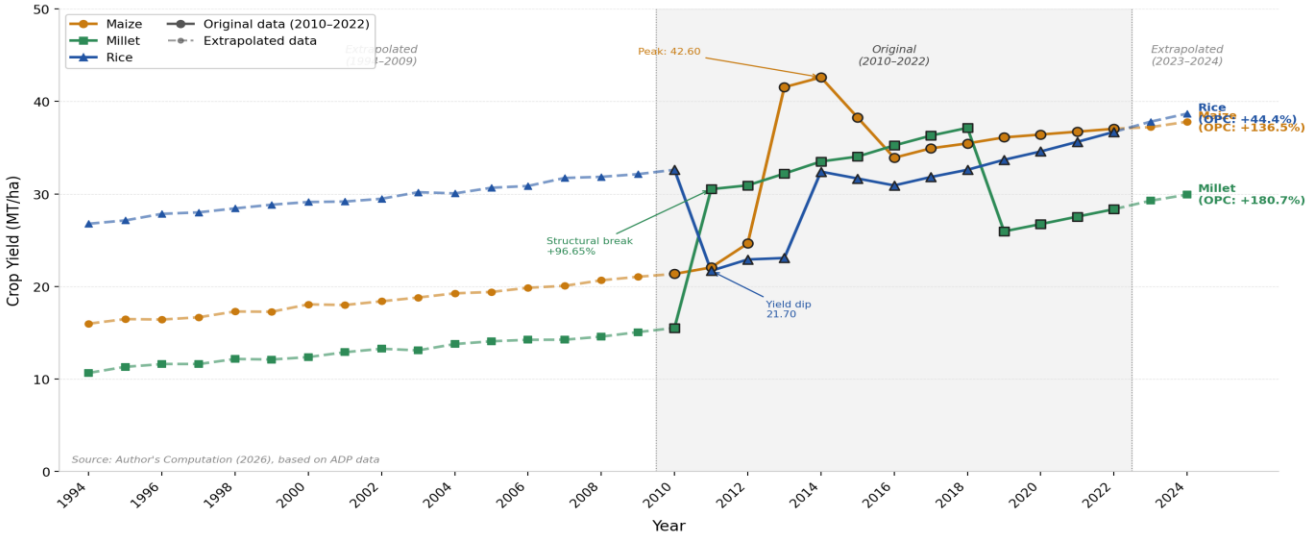

Figure 2: Crop yield trend lines (1994–2024)

These patterns show that all three crops improved substantially over time, but they did so at different rates and with different levels of stability. Millet appears to have responded most strongly to the changing peri-urban environment, while rice remained more consistent but less dynamic.

4.2 Climate-Crop Relationships

To characterize the climatic regime and detect systematic long-term shifts across the 31-year operational timeline in Gwagwalada Area Council, non-parametric statistical evaluations were executed on the continuous annual meteorological series. The summary parameters of the Mann-Kendall trend test and Sen's slope estimation are presented in Table 2.

Table 2: Mann-Kendall Trend Test and Sen's Slope Parameter Estimates (1994–2024)

Climate Variable	Mann-Kendall Score (Z)	Sen's Slope (β)	p-value
Annual Rainfall	-1.43	-10.49 mm/year	0.153 (ns)
Annual Mean Temperature	+2.48	+0.037°C/year	0.013*

*Note: * indicates statistical significance at the 95% confidence level ($p < 0.05$); ns indicates non-significance.*

Rainfall exhibited a non-significant trend ($Z = -1.43$; $p = 0.153$; $\beta = -10.49$ mm/year), indicating that no statistically significant directional change in annual rainfall was detected over the study period. Mean temperature, by contrast, showed a statistically significant increasing trend ($Z = +2.48$; $p = 0.013$; $\beta = +0.037$°C/year), confirming cumulative warming of approximately 1.14°C across the 31-year record.

Table 3 shows the summary of the correlation results for all three crops (maize, millet, and rice) with the climate variables (rainfall and temperature) from 1994 to 2024. Pearson correlation analysis shows that rainfall had weak, negative, and statistically non-significant relationships with maize, millet, and rice yields ($r = -0.2927$, -0.2763, and -0.1069, respectively; $p > 0.05$).

Table 3: Summary of Pearson Correlation Results: Crop Yield vs. Climate Variables (1994–2024)

Crop	RF r	RF r^2	RF p-value	Temp r	Temp r^2r^2	Temp p-value
Maize	-0.2927	0.0857	0.1101 (ns)	0.4426	0.1959	0.0127
Millet	-0.2763	0.0763	0.1325 (ns)	0.3709	0.1376	0.0400
Rice	-0.1069	0.0114	0.5671 (ns)	0.4417	0.1951	0.0129

In the full 31-year series, temperature showed positive correlations with maize, millet, and rice, with the corresponding p-values below 0.05. However, these associations were not statistically significant in the verified 2010–2022 window, so the full-series significance results should be interpreted cautiously, with *r* values of 0.443, 0.371, and 0.442, respectively. This means that within the observed range, warmer years were generally associated with higher crop yields.

Multiple regression results reinforce the same pattern. Multiple linear regression models were estimated for each crop with annual rainfall and mean temperature as predictors and crop yield as the outcome variable (n = 31). Table 4 presents the regression coefficients, model fit statistics, and significance values.

Table 4: Multiple Regression Results: Crop Yield ~ Annual Rainfall + Mean Temperature (n = 31)

Statistic	Maize	Millet	Rice
R^2	0.1959 (19.6%)	0.1396 (14.0%)	0.2523 (25.2%)
Adjusted R^2R^2	0.1385	0.0781	0.1989
F-statistic F (2,28)	3.411	2.272	4.724
Model p- value	0.047	0.122 (ns)	0.017
β Rainfall	-0.0002	-0.0017	+0.0037
p-value (rainfall)	0.976 (ns)	0.798 (ns)	0.154 (ns)
β Temperature	+5.605	+4.334	+3.522
P-value (Temperature)	0.060	0.1652 (ns)	0.006

Table 5 presents the variance partitioning results, decomposing the combined R^2 into the unique contributions of each climate variable and their shared explanatory component.

Table 5: Variance Partitioning: Unique and Shared Contributions of Rainfall and Temperature to Crop Yield Variance

Variance component	Maize (%)	Millet (%)	Rice (%)
Unique contribution of rainfall	0.00	0.20	5.72
Unique contribution of Temperature	11.02	6.33	24.09
Shared variance (RF + Temp)	8.56	7.43	0.00
Total explained (combined R^2)	19.59	13.96	25.23
Unexplained variance	80.41	86.04	74.77

Combined rainfall and temperature explained only a modest share of yield variation, with R^2 values ranging from 14.0 percent to 25.2 percent, and temperature emerging as the dominant predictor. Figure 3 illustrates the variance partitioning for all three crops.

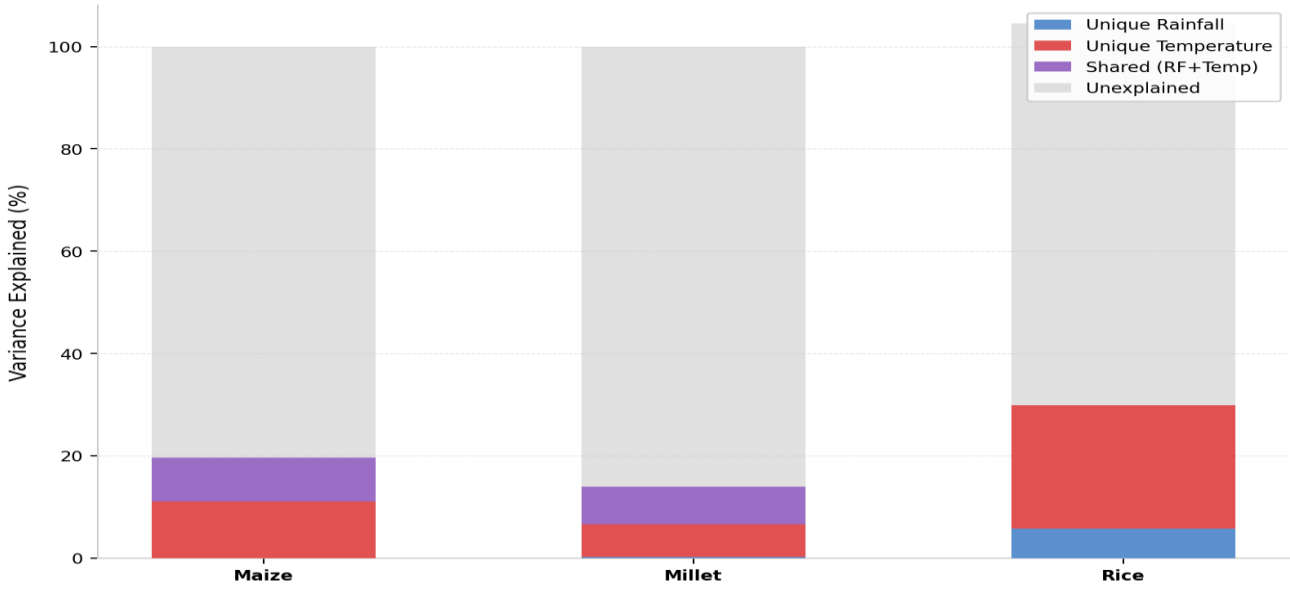

Figure 3: Variance Partitioning

That leaves 74.8 percent to 86.0 percent of yield variation unexplained by climate variables alone, which supports the argument that non-climatic factors, especially urbanisation-linked changes, played a larger role.

Because 18 of the 31 crop-yield observations were extrapolated, the climate–crop statistical analyses were re-run using only the verified Agricultural Development Project records for 2010–2022 (n = 13). The direction of all climate–yield associations was consistent between the full 31-year series and the verified 2010–2022 window, although statistical significance was not achieved in the shorter window, likely reflecting reduced statistical power at n = 13. The full-series results are therefore retained as the principal descriptive analysis but must be interpreted with explicit recognition that 18 of the 31 observations are extrapolated. Table 6 presents the comparison between the climate variables and the crop yield for the full years and the verified data.

Table 6: Pearson Correlation: Climate Variables vs Crop Yield — Full Series (n = 31) and Verified Window (n = 13) Comparison

Variable / Crop	Full Series (n = 31)		Verified Window (n = 13)		Remarks / Comparison
	R	p-value	R	p-value	
Maize–Rainfall	-0.293	0.110 (ns)	+0.084	0.786 (ns)	Direction reverses; both non-significant
Maize–Temperature	+0.443	0.013 *	+0.452	0.121 (ns)	Direction consistent; significance lost at n=13
Millet–Rainfall	-0.276	0.133 (ns)	-0.285	0.345 (ns)	Direction consistent; both non-significant
Millet–Temperature	+0.371	0.040 *	+0.475	0.101 (ns)	Direction consistent; significance lost at n=13
Rice–Rainfall	-0.107	0.567 (ns)	+0.668	0.013 *	Direction reverses; significant in verified window
Rice–Temperature	+0.442	0.013 *	-0.219	0.473 (ns)	Direction reverses; both non-significant

Note. *ns = not significant (p > 0.05); * p < 0.05. The n=13 window covers the verified original ADP data (2010–2022) only, excluding all extrapolated observations.*

Several important patterns emerge from the robustness check. First, all relationships that were non-significant in the full series remain non-significant in the verified window, confirming the absence of rainfall effects on maize and millet yield regardless of the data window used. Second, the temperature-yield associations for maize and millet that were significant in the full series (p = 0.013 and p = 0.040, respectively) lose statistical significance in the verified window (p = 0.121 and p = 0.101). This indicates that the significance of these associations in the full series was at least partly dependent on the extrapolated observations, and these results should therefore be described as directionally consistent but not robustly confirmed under verified data alone. Third, the most notable change involves rice: the negative rainfall correlation in the full series (r = −0.107; ns) reverses to a positive and significant relationship in the verified window (r = +0.668; p = 0.013), suggesting that during the

actual observed period (2010–2022), higher rainfall was associated with higher rice yield, a result that is more agronomically intuitive and may have been masked in the full series by the extrapolated trend in earlier years.

Table 7 shows the combined multiple regression for Crop yield, Annual rainfall, and mean temperature for the full 31 years (n=31) and the original years (n =13).

Table 7: Multiple Regression Results: Crop Yield ~ Annual Rainfall + Mean Temperature – Full Series (n = 31) vs Verified Window (n = 13)

Crop	Full Series (n = 31)				Verified Window (n = 13)			
	R^2	Adj. R^2	F-stat	p-value	R^2	Adj. R^2	F-stat	p-value
Maize	0.1959 (19.6%)	0.1385	3.411	0.047 *	0.3206 (32.1%)	0.1847	2.359	0.145 (ns)
Millet	0.1396 (14.0%)	0.0781	2.272	0.122 (ns)	0.2301 (23.0%)	0.0762	1.495	0.270 (ns)
Rice	0.2523 (25.2%)	0.1989	4.724	0.017 *	0.4588 (45.9%)	0.3506	4.239	0.046 *

*Note. k = 2 predictors (Rainfall and Temperature) in all models. df = (2, 28) for n=31; df = (2, 10) for n=13. * p < 0.05; ns = not significant.*

The multiple regression results show both convergence and divergence between the two windows. For millet, the model is non-significant in both windows, confirming that combined climate variables do not reliably explain millet yield variation in either dataset. For rice, the model is significant in both windows (p = 0.017 in the full series; p = 0.046 in the verified window), with R^2 actually increasing from 25.2% to 45.9% in the verified data, driven by the strong positive rainfall-Rice relationship identified in Table 6. Notably, however, in the verified window it is rainfall (b = 0.0167; p = 0.020) rather than temperature (b = 1.189; p = 0.635) that is the significant predictor of rice yield, reversing the pattern seen in the full series. For maize, the full-series model is significant (p = 0.047) while the verified-window model is not (p = 0.14). These results collectively indicate that the climate-yield findings should be interpreted with appropriate caution as directional evidence rather than robustly confirmed statistical relationships.

Table 8 shows the combined variance partitioning for the unique and shared contributions of rainfall and temperature for the full years (n=31) and the original years (n=13).

Table 8: Variance Partitioning: Unique and Shared Contributions of Rainfall and Temperature – Full Series (n = 31) vs Verified Window (n = 13)

Component	Maize		Millet		Rice	
	Full (n=31)	Verified (n=13)	Full (n=31)	Verified (n=13)	Full (n=31)	Verified (n=13)
Unique Rainfall	0.00	11.62	0.20	0.44	5.72	41.10
Unique Temperature	11.02	31.36	6.33	14.89	24.09	1.30
Shared (RF + Temp)	8.56	-10.92	7.43	7.69	0.00	3.48
Total Explained (R^2)	19.59	32.06	13.96	23.01	25.23	45.88
Unexplained	80.41	67.94	86.04	76.99	74.77	54.12

Note. *Negative shared variance (Maize n=13: -10.92%) arises when the two predictors are negatively correlated with each other in the verified window, a mathematical outcome of the suppression effect between Rainfall and Temperature across the 2010–2022 period. This does not represent a data error but indicates that the two predictors partially suppress each other's explanatory contribution in this shorter window.*

The variance partitioning results reinforce the pattern identified in Tables 6 and 7. For maize, the role of temperature as the dominant climate predictor is consistent across both windows (unique contribution 11.02% at n=31; 31.36% at n=13), though the negative shared variance (−10.92%) in the verified window indicates a suppression relationship between rainfall and temperature in the 2010–2022 period. For millet, temperature remains the dominant climate contributor in both windows (6.33% at n = 31; 14.89% at n = 13). For rice, the most striking change is the shift from temperature as the dominant contributor in the full series (24.09%) to rainfall as the dominant contributor in the verified window (41.10%), confirming that the observed rice-rainfall relationship is a genuine feature of the original data period rather than an artefact of the full-series extrapolation. In both windows, unexplained variance remains the largest component for all crops (54.12%–86.04%), confirming that non-climatic factors, principally urbanisation-associated agricultural intensification, account for the dominant share of yield variation regardless of which data window is used. This finding is robust across both series and does not depend on the extrapolated observations.

4.3 Urbanisation-Crop Relationships

Based on the Global Human Settlement Layer framework,

the classified epochs captured three distinct milestones: 1994 (Class 1: rural), 2004 (Class 2: peri-urban), and 2024 (Class 5: high-density urban core).

Table 9 presents the combined epoch-level picture, integrating urbanisation class, rainfall, temperature, and crop yields for the three classified LULCC epochs. The epoch-level synthesis reveals a coherent compound narrative that summarises the epoch-level comparison of built-up area, temperature, and crop yield.

Table 9: Epoch-Level Combined Summary: Urbanisation Class, Rainfall, Temperature, and Crop Yields

Epoch	Built-up (sq km)	Urban class	Rainfall (mm)	Temp (℃)	Maize (MT/ha)	Millet (MT/ha)	Rice (MT/ha)
1994	58.82	Class 1	1,922.9	24.77	15.98	10.66	26.78
2004	107.89	Class 2	863.8	26.67	19.26	13.78	30.06
2024	203.33	Class 5	971.1	27.04	37.80	29.92	38.68

In 1994 (Class 1, Very low-density rural), the study area experienced the highest recorded rainfall of any epoch year (1,922.9 mm) and the coolest temperatures (24.77°C), yet recorded the lowest yields for all three crops (Maize: 15.98; Millet: 10.66; Rice: 26.78 MT/ha). This suggests that abundant rainfall alone was insufficient to drive productivity.

In 2024 (Class 5, Very high-density urban), rainfall had partially recovered to 971.1 mm, and temperature stood at 27.04°C, the highest of the three epochs. All three crops recorded their highest observed yields (Maize: 37.80; Millet: 29.92; Rice: 38.68 MT/ha).

By 2004 (Class 2, Low-density peri-urban), rainfall had fallen dramatically to 863.8 mm, the lowest of the three epoch years, while temperature had risen to 26.67°C. Despite the drier conditions, all three crop yields increased (Maize: +20.5 percent; Millet: +29.3 percent; Rice: +12.3 percent).

Table 10 represents the statistical synthesis of urbanisation relationships across the classified epochs (n= 3), for all three crops using Spearman rank, the derived yield-per-urbanisation rate (r_u), and the simple linear regression (urbanisation as independent variables and crops as the dependent variable). Relationship analysis using non-parametric Spearman rank correlation indicated perfect positive co-movement between urbanisation extent and the yields of all three cereals, as well as between urbanisation extent and annual mean temperature, across the three classified milestones ([n = 3]). Because the analysis is based on only three structural observations, these results should not be interpreted as statistically robust evidence of causation.

Table 10: Statistical Synthesis of Urbanisation Relationships across Classified Epochs (n = 3)

Dependent Variable (Y)	Spearman Rank (rs)	Urbanisation Rate (ru)	Regression Intercept (a)	Regression Slope (b)	Model Fit (R^2)
Maize Yield (MT/ha)	1.00	0.1510	4.993	0.1569	0.960
Millet Yield (MT/ha)	1.00	0.1333	1.077	0.1382	0.965
Rice Yield (MT/ha)	1.00	0.0823	21.548	0.0834	0.995
Mean Temperature (°C)	1.00	—	—	0.0141	0.918

**Note: The temperature intercept is an unobservable mathematical constant and is excluded. Due to severe sample size constraints (n = 3, dfresidual = 1), parametric p-values and significance tests are omitted, and outputs function strictly as descriptive trend trajectories rather than causal inferences.*

To quantify this spatial co-movement, the derived yield-per-urbanisation rate *(ru)* demonstrated that maize had the highest sensitivity to expanding built footprints at 0.1510 MT/ha per square kilometre, followed by millet at 0.1333 MT/ha per square kilometre and rice at 0.0823 MT/ha per square kilometre. To formalise the descriptive magnitude and linear fit of these structural shifts, simple linear regression models were executed across the epochs. Crucially, because these models were fitted strictly across the three classified LULC milestones (n = 3), the residual degrees of freedom were limited to one (dfresidual = 1). Consequently, these models are presented strictly as descriptive trend trajectories and measures of linear co-movement rather than tools for parametric significance testing; as p-values are not statistically interpretable at this sample size, no significance tests are reported, and the outputs must not be interpreted as evidence of a causal relationship. Figure 4 shows built-up area and crop yield; built-up area and temperature, on a dual-axis chart across the three epochs.

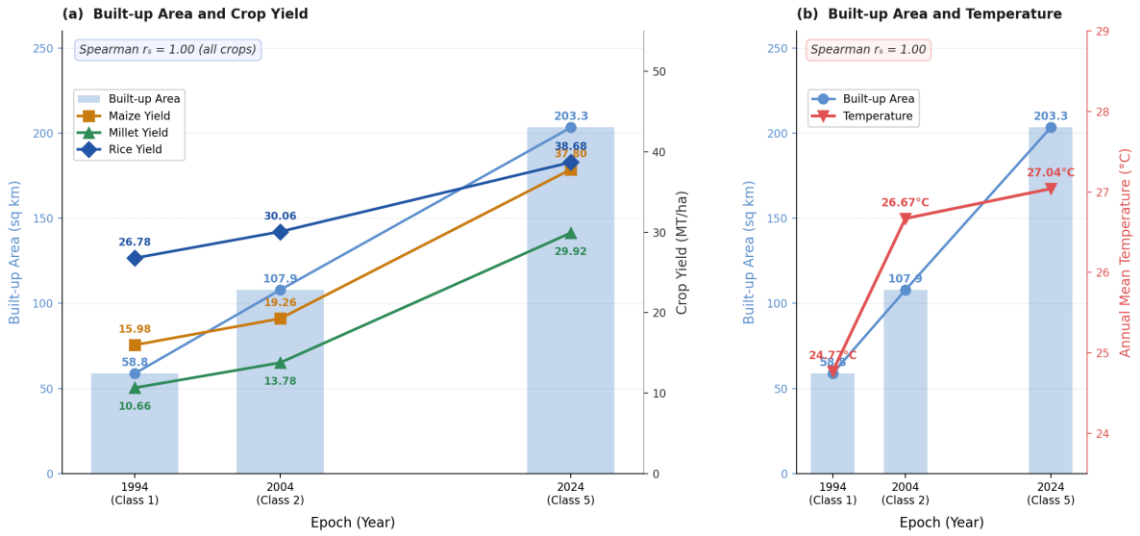

Figure 4: Built-up Area and Crop Yield, Built-up Area and Temperature across the Three Epochs.

The agricultural descriptive regression models yielded high coefficients of determination across the three classified milestones. These values indicate close structural alignment among the three observations, but they should not be interpreted as evidence that urbanisation caused the observed yield increases. Rice recorded the highest descriptive linear fit (R^2 = 0.995, intercept a = 21.548, slope b = 0.0834), followed closely by millet (R^2 = 0.965, intercept a = 1.077, slope b = 0.1382) and maize (R^2 = 0.960, intercept a = 4.993, slope b = 0.1569). The larger descriptive slope coefficient for maize indicates a stronger observed co-movement with built-up area across the three classified epochs; it should not be interpreted as evidence of a causal response to urbanisation. Rice proved to be the most structurally stable but least dynamic crop. This descriptive co-movement is compatible with contributions from non-climatic factors such as enhanced market access, input intensification, and management change, but the available evidence does not allow their individual effects to be isolated.

Parallel to the crop metrics, the descriptive simple linear regression of annual mean temperature on built-up area, as shown in Figure 4 produced a positive slope (b = 0.0141) and a strong linear fit (R^2 = 0.918), indicating an estimated increase of approximately 0.014 °C in annual mean temperature for each additional square kilometre of built-up area across the three aligned epochs. Adhering to the same baseline constraints, this temperature model serves strictly as a descriptive estimate of temperature change associated with increasing built-up area and cannot be used to establish a causal urban heat-island effect or definitive local causation. Instead, these synchronized values outline a coherent localized trajectory where physical urban growth and environmental temperature parameters expanded in tandem.

Figure 5 presents the same epoch-level synthesis as Table 9 in indexed form, setting 1994 = 100 for all five variables to enable proportional comparison across the study period. The synthesis of Figure 5 and Table 9, permits a holistic assessment of how urbanisation and climate conditions jointly characterised each yield period.

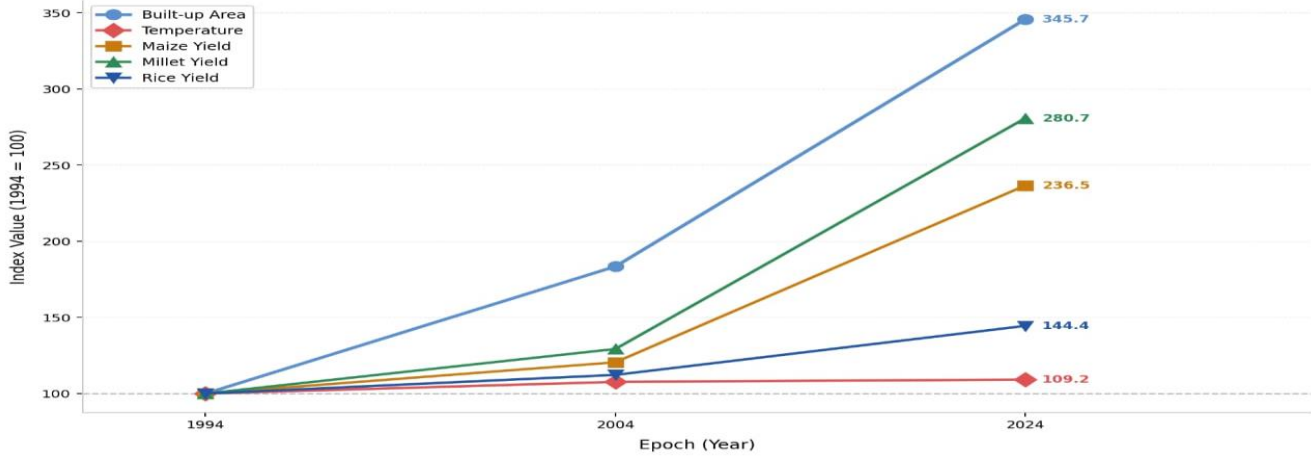

Figure 5: Combined index chart (Built-up, Temp, all crops — 1994=100)

4.4 2050 Simulation Results

To evaluate the structural transformations characterising the Gwagwalada landscape over the 31-year study period, multitemporal remote sensing datasets were synthesised across three historical milestones. Figure 6 illustrates the spatiotemporal maps of Gwagwalada Area Council displaying the independent land classes, which reveal the patterns of physical urban growth alongside the concurrent contraction of the agricultural land base, across three historical milestones: (a) 1994, (b) 2004, and (c) 2024.

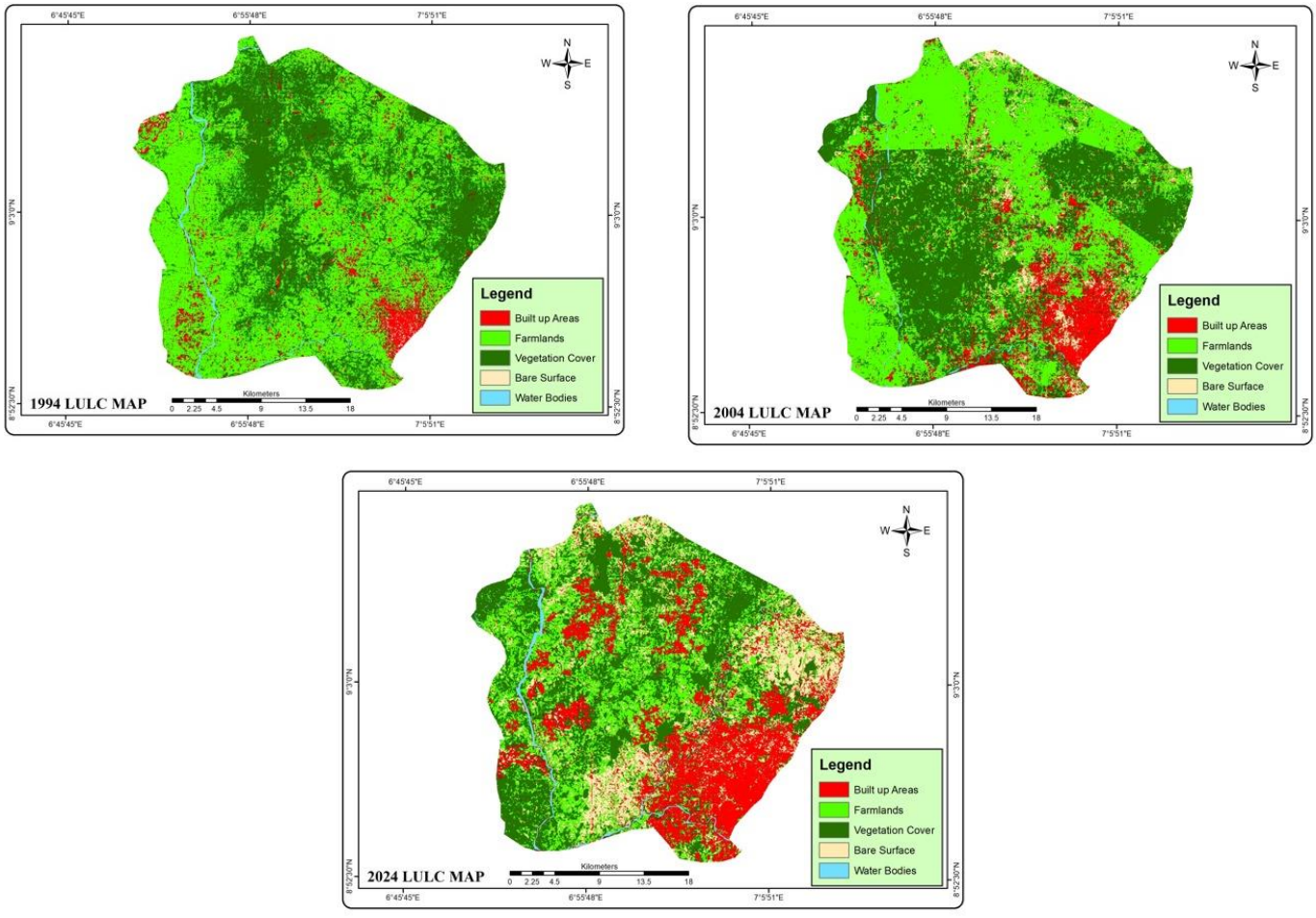

Figure 6: Spatiotemporal Classified LULCC Maps of Gwagwalada for 1994, 2004 and 2024

Visual inspection of the classified epochs reveals a pronounced centrifugal expansion of built-up areas outward from the urban core, encroaching heavily upon the surrounding low-density peri-urban fringe. This spatial trajectory is characterized by a rapid, systemic landscape conversion, wherein the built-up area expanded from a baseline of 58.82 km² in 1994 to a high-density core of 203.33 km² by 2024. Crucially, this physical intensification did not unfold uniformly across the territory; rather, it initiated a severe structural reorganisation of the landscape, displacing prime agricultural fields and capturing a major share of temporal land cover variation prior to the execution of the 2050 forward-simulated modeling framework.

Table 11 shows the LULC area distribution and change dynamics for the study area for five land cover classes (Built-up Area, farmland, vegetation, Bare surface, and water bodies) from 1994 - 2024.

Table 11: Land Use and Land Cover (LULC) Area Distribution and Change Dynamics in Gwagwalada Area Council (1994–2024)

LULC Class	1994 Extent (Sq Km)	2004 Extent (Sq km)	2024 Extent (Sq km)	Net Change 1994-2024 (sq km)	Total Percentage Change (%)
Built-up Area	58.82	107.89	203.33	+144.51	+245.68
Farmland	536.04	450.41	278.11	-257.93	-48.12%
Vegetation	302.07	300.24	251.33	-50.74	-16.80%
Bare Surface	6.60	48.93	165.68	+159.08	+2410.30
Water Bodies	8.46	4.51	13.43	+4.97	+58.75%
Total Area	**911.99**	**911.98**	**911.89**	**-0.11**	**-0.01%**

Between 1994 and 2024, water bodies increased from 8.46 km² to 13.43 km² (+58.75%), following an initial decline to 4.51 km² in 2004. This post-2004 expansion is driven by infrastructural expansions at the Lower Usuma Dam and a near-doubling of impervious built-up areas (107.89 km² to 203.33 km²). The loss of natural land cover accelerated stormwater runoff into low-lying floodplains, creating artificial ponding and wider river channels detected by Landsat sensors (Achugbu et al., 2022; Idowu & Zhou, 2021). Furthermore, a significant reduction in dense riparian vegetation along the riverbanks stripped away the natural canopy cover, exposing previously hidden water surfaces directly to the satellite sensors. Coupled with minor seasonal variations in image acquisition dates, this trend reflects rapid urban development and landscape exposure rather than natural environmental recovery.

Table 12 shows the accuracy assessment for 1994, 2004, and 2024. The study used 250 randomly selected reference points for each classified epoch. The points were independently checked against available historical imagery, including Google Earth Pro imagery where applicable.

Table 12: Accuracy Assessment Table

Epoch Milestone	Overall Accuracy (%)	Kappa Statistic (Kc)	Verification Points (n)
1994 Baseline	81.30	0.79	250
2004 Transition	82.20	0.8	250
2024 Modern Core	83.50	0.82	250

According to established remote sensing benchmarks, an overall classification accuracy exceeding 80% and a corresponding Kappa coefficient above 0.70 represent an excellent level of agreement between the classified satellite imagery and ground-truth parameters (Rawat & Kumar, 2015; Rwanga & Ndambuki, 2017). Consequently, the baseline data layers demonstrate sufficient thematic structural integrity to serve as reliable inputs for the CA-Markov forward-simulated spatial modeling framework.

Table 13 presents the projected land use and land cover change of Gwagwalada for the year 2050, alongside the 2024 baseline, for the five land cover classes (Built-up Areas, Farmlands, Vegetation, Bare surface and Water bodies). The CA-Markov simulation projected built-up area to increase to 351.72 sq km by 2050, representing a 72.98 percent rise from the 2024 baseline.

Table 13: Simulated LULC Change: 2024 Baseline and 2050 Projection

LULC Class	2024 Extent (sq km)	2050 Extent (sq km)	Magnitude of change (sq km)	Percentage of Change	Annual Rate of Change (percent)
Built-up areas	203.33	351.72	148.39	72.98	2.81
Farmlands	278.11	212.34	-65.77	-23.65	-0.91
Vegetation	251.33	238.62	-12.71	-5.06	-0.19
Bare surface	165.68	96.05	-69.64	-42.03	-1.62
Water Bodies	13.43	13.05	-0.38	-2.83	-0.11

Farmland is projected to decline to 212.34 sq km, a reduction of 23.65 percent relative to 2024. These changes indicate continued urban pressure on agricultural land even though the area will still retain a meaningful farming base by 2050.

Figure 7 shows the projected land use and land cover change map of Gwagwalada for the year 2050

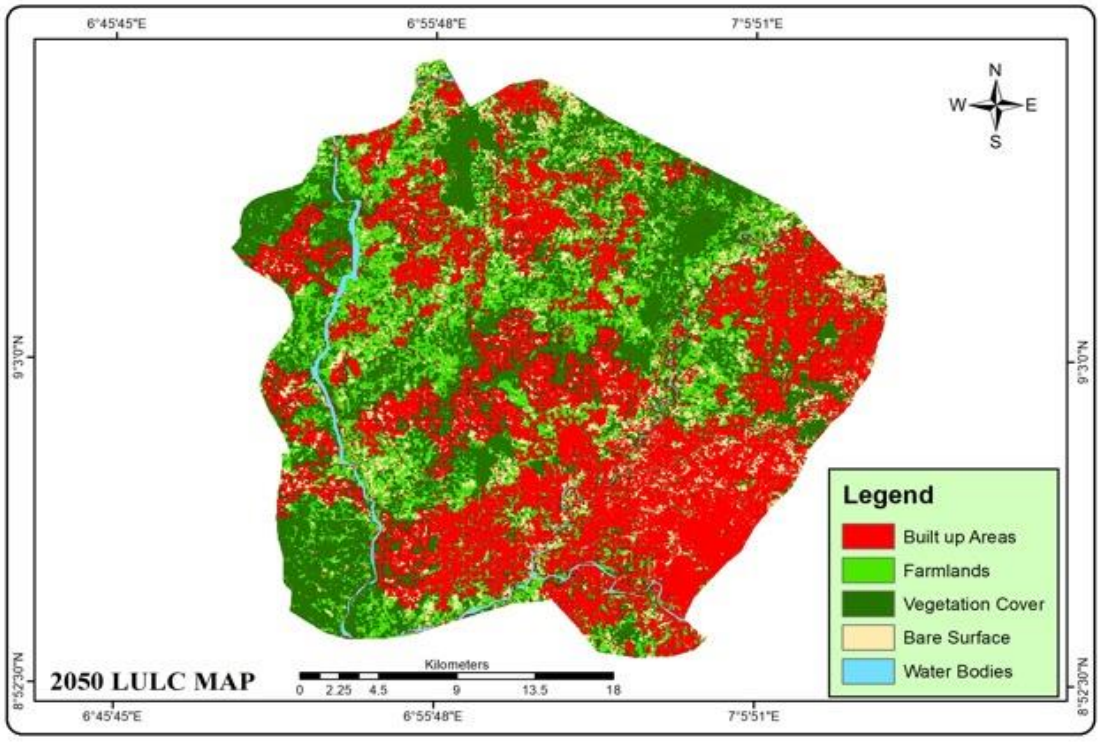

Figure 7: Projected 2050 LULCC Map of Gwagwalada

Table 14 presents the revised estimated total production of maize, millet, and rice for 2024 and the projected total production under the 2050 urbanisation scenario, together with the percentage change in production between the two periods.

Table 14: Scenario-Based Revised Crop Production Estimates for 2024 and 2050

Crop	Revised 2024 Total (MT)	Revised 2050 Total (MT)	Change
Maize	420,504	511,372	+21.6%
Millet	367,203	465,364	+26.8%
Rice	268,900	270,147	+0.5%

The projections indicate that total production is expected to increase for all three crops despite the anticipated reduction in available farmland. Maize production is projected to rise from 420,504 MT in 2024 to 511,372 MT by 2050, representing a 21.6% increase. Millet records the largest proportional increase, rising from 367,203 MT to 465,364 MT, equivalent to a 26.8% increase. Rice production changes only marginally, increasing from 268,900 MT in 2024 to 270,147 MT in 2050, or 0.5%. This near-static outcome suggests that projected yield gains for rice may largely offset the effects of farmland reduction, leaving little overall increase in aggregate production.

Overall, the table indicates that maize and millet may experience stronger production growth under the 2050 scenario, whereas rice appears more constrained and vulnerable to the loss of agricultural land. These figures should be interpreted as scenario-based estimates rather than definitive forecasts, because they depend on the assumed continuation of historical yield relationships, urbanisation trends, and crop-specific farmland allocation.

5 Discussion

The findings indicate that non-climatic factors may have contributed substantially to the observed yield patterns, although the available data do not permit firm attribution of causality. Built-up land expanded sharply from 58.82 km² in 1994 to 203.33 km² in 2024, while farmland declined from 536.04 km² to 278.11 km². At the same time, maize, millet, and rice yields increased, showing that productivity improved even as farmland shrank. This means the key change is structural: agriculture is being reorganised under urban pressure rather than simply declining in output. Climate variables explained only 14.0% to 25.2% of yield variance, suggesting that a significant portion of the change is linked to non-climatic forces such as land conversion, fragmentation, and intensification. Similar patterns have been reported in peri-urban Africa by Hu et al. (2025) and Degefu and Kifle

(2024), where urban expansion reduces farmland and weakens food availability. The Gwagwalada findings are consistent with wider literature showing that peri-urban crop systems reflect the combined influence of urban expansion, land-use change, market access, management practices, and climate variability. The present analysis does not establish that urban growth was more influential than climate variability.

In the full series, temperature showed stronger positive associations with all three crops than rainfall; however, these associations were not statistically significant in the verified-data-only analysis. This finding is in agreement with Eck et al. (2020), Gashure (2025), and Bitew and Minale (2026). A likely explanation is that slightly warmer conditions may have supported crop growth or extended the effective growing season, especially where farmers adapted through better management.

Rainfall was not significant because annual totals do not capture rainfall timing, dry spells, or onset problems, which are more important for rainfed crops. Management changes and urban-related confounding likely weakened the rainfall signal further. This pattern echoes findings from Akinseye et al. (2012) in Nigeria, Ankrah et al. (2023) in Ghana, and Mubenga-Tshitaka et al. (2023) in East Africa.

Rice had the lowest r_u value, meaning its yield gains were least able to offset farmland loss. Although rice was the most stable crop, its projected total production change by 2050 is near-static, at only +0.5 percent. This shows that stable per-hectare yield does not guarantee stable total output when farmland keeps shrinking. In practical terms, rice illustrates how land loss can cancel productivity gains.

Ningi et al. (2025) found that climate variability exerted significant and differential impacts on field-crop production systems in South Africa over a 45-year period, with production stability linked more strongly to accumulated multi-year climate patterns than to individual seasonal conditions. This finding is consistent with the observation in Gwagwalada that annual rainfall totals alone do not reliably explain year-to-year crop-yield outcomes.

The robustness check confirms three key conclusions that are stable across both data windows. First, combined climate variables explain only a modest share of yield variance in both windows, between 13.96% and 45.88%, leaving the majority of yield variability attributable to non-climatic factors. Second, the direction of the temperature-yield associations is consistent in both windows for maize and millet, though significance is not achieved in the verified window due to reduced statistical power at n = 13. Third, and most notably, Rice yield shows a significantly positive relationship with rainfall in the verified window ($r = +0.668$; $p = 0.013$), which is more agronomically intuitive than the non-significant negative association found in the full series, suggesting that the full-series rainfall-rice result was partly shaped by the extrapolated early years. These findings reinforce the primary conclusion of the study while introducing appropriate nuance: the positive temperature-yield associations reported for maize and millet should be described as directionally consistent but not robustly confirmed, while the positive rainfall-rice association is a genuine feature of the original observed data.

The descriptive simple linear regression models revealed a strong positive co-movement between built-up area and per-hectare crop yields across the three epochs in Gwagwalada Area Council. However, this localized pattern operates within a complex socio-ecological framework and must be contextualized against a substantial body of global empirical evidence demonstrating that urbanisation typically impairs agricultural systems. While the high descriptive coefficients of determination (R^2) and positive slopes in this study indicate that urban growth captured a major share of temporal yield variation, wider global literature frequently documents severe landscape degradation, agricultural fragmentation, and a contraction of long-term crop production potential under urban expansion (Bren d'Amour et al., 2017; Huang et al., 2020). For example, regional assessments from the North China Plain establish that aggressive urban expansion triggers significant aggregate crop yield losses (Sheng & Huang, 2025). Furthermore, contemporary landscape modelling shows that as urbanisation intensity rises and impervious surfaces expand, agricultural yield potential systematically declines (Meng et al., 2025). This stark divergence highlights that the urbanisation-yield nexus is highly context-specific. In Gwagwalada, short-term yield gains concurrent with urban expansion likely reflect peri-urban intensification, enhanced proximity to urban markets, and strategic farmer adaptations. This dynamic is corroborated by specific peri-urban studies demonstrating that urban growth can actively coincide with more intensive cultivation techniques, improved regional market connectivity, and higher-input production systems in the Global South (Boudet et al., 2020; Berkum, 2023). Nonetheless, global evaluations warn that the land absorbed by expanding cities often encompasses a region's most fertile and productive topsoil (Andrade et al., 2022). Consequently, urban growth frequently displaces premier agricultural zones, masking localized, short-term per-hectare yield gains with a hidden, structural erosion of the broader agricultural resource base (Estrada et al., 2017).

The main planning implication is that farmland-

protection zoning represents a sensible and evidence-informed precaution for sustaining agricultural capacity to 2050. The CA-Markov results indicate continued built-up expansion and farmland decline; consequently, the protection of strategic agricultural areas warrants consideration within ongoing revisions of the FCT Master Plan.

6 Conclusion

This study demonstrates a strong, descriptive positive association between built-up area expansion and the per-hectare yields of maize, millet, and rice across the 1994, 2004, and 2024 milestones in Gwagwalada Area Council. The findings indicate that non-climatic factors may have contributed substantially to the observed yield patterns, although the available data do not permit firm attribution of causality. Crucially, when evaluated against global empirical evidence where urban sprawl directly undermines food security through cropland fragmentation and high-value soil displacement, these findings do not signal a permanent, harmonious relationship (Bren d'Amour et al., 2017; Huang et al., 2020). The observed and projected conversion of fertile fields indicates that despite rising short-term per-hectare productivity, continued built-up area expansion poses an acute, long-term threat to Gwagwalada's foundational agricultural base. Sustainable food security will require strategic land-use planning that protects core agricultural zones within the expanding Federal Capital Territory.

The ru metric provides a simple descriptive tool for peri-urban projection in data-limited settings. When combined with CA-Markov modelling, it offers a practical framework for exploring how alternative urban-growth scenarios may affect crop yields and aggregate production. The findings therefore support consideration of farmland protection, stronger land-use control, and the inclusion of agricultural-land scenarios in ongoing FCT Master Plan revision, while recognising that these recommendations are precautionary and should not be interpreted as direct causal conclusions from the present analysis.

References

Achugbu, I. C., Olufayo, A. A., Balogun, I. A., Dudhia, J., McAllister, M., Adefisan, E. A., & Naabil, E. (2022). Potential effects of land use land cover change on streamflow over the Sokoto Rima River Basin. Heliyon, 8(7), e09779. https://doi.org/10.1016/j.heliyon.2022.e09779

Aina, H. O., & Sule, A. (2025). Environmental and health implications of waste management deficiency in Gwagwalada Town, FCT, Nigeria. International Journal of Research and Innovation in Social Science (IJRISS), 9(9), 104. https://doi.org/10.47772/IJRISS.2025.909000104

Akinseye, F. M., Ogunjobi, K. O., & Okogbue, E. C. (2012). Climate variability and food crop production in Nigeria. International Journal of Academic Research Part A, 4(5), 107–111. https://doi.org/10.7813/2075-4124.2012/4-5/A.13

Amaechi, C. F., & Hassan, S. M. (2022). Risk assessment of climate variability in the Federal Capital Territory, Abuja, Nigeria. Nigerian Institution of Professional Engineers and Scientists Journal of Science and Technology Research, 4(1), 90–105. https://doi.org/10.37933/nipes/4.1.2022.8

Andrade, J. F., Cassman, K. G., Rattalino Edreira, J. I., Agus, F., Bala, A., Deng, N., & Grassini, P. (2022). Impact of urbanization trends on production of key staple crops. Ambio, 51(5), 1158–1167. https://doi.org/10.1007/s13280-021-01674-z

Aniekwe, S., & Igu, N. I. (2022). A geographical analysis of urban sprawl in Abuja, Nigeria. Journal of Geography Research, 2(1), 12–18. https://doi.org/10.30564/jgr.v2i1.344

Ankrah, D., Okyere, C., Mensah, J., & Okata, E. (2023). Effect of climate variability adaptation strategies on maize yield in the Cape Coast Municipality, Ghana. Cogent Food & Agriculture, 9(1), Article 2247166. https://doi.org/10.1080/23311932.2023.2247166

Berkum, S. V. (2023). How urban growth in the Global South affects agricultural dynamics and food systems outcomes in rural areas: A review and research agenda. Sustainability, 15(3), Article 2591. https://doi.org/10.3390/su15032591

Bitew, A. B., & Minale, A. S. (2026). Spatio-temporal dynamics of climate variability and its impact on major crop yields across different agro-ecological zones of the Ayehu watershed, Northwest Ethiopia. Discover Sustainability, 7, Article 110. https://doi.org/10.1007/s43621-025-02501-1

Bonan, G. (2015). Climate variability. In Ecological climatology: Concepts and applications (pp. 103–116). Cambridge University Press. https://doi.org/10.1017/CBO9781107339200.008

Boudet, F., MacDonald, G. K., Robinson, B. E., & Samberg, L. H. (2020). Rural-urban connectivity and agricultural land management across the Global South. Global Environmental Change, 60, Article 101982. https://doi.org/10.1016/j.gloenvcha.2019.101982

Bren d'Amour, C., Reitsma, F., Baiocchi, G., Barthel, S., Güneralp, B., Erb, K., Haberl, H., Creutzig, F., & Seto, K. C. (2017). Future urban land expansion and implications for global croplands. Proceedings of the National Academy of Sciences of the United States of America, 114(34), 8939–8944. https://doi.org/10.1073/pnas.1606036114

Chunwate, B. T., Yerima, S. Y., & Ademu, S. (2021). Analysis of land-use conflict between farmers and pastoralists in Gwagwalada Area Council of Abuja, Nigeria. Global Journal of Science Frontier Research: H Environment & Earth Science, 21(3), 49–55. https://journalofscience.org/index.php/GJSFR/article/view/2952

Cobbinah, P. B. (2023). City in Africa II: Urban environmental health. Journal of Urban Affairs. Advance online publication.

https://doi.org/10.1080/07352166.2023.2171617

Conover, W. J. (1999). Practical nonparametric statistics (3rd ed.). John Wiley & Sons.

Degefu, M. A., & Kifle, F. (2024). Impacts of climate variability on the vegetable production of urban farmers in the Addis Ababa metropolitan area: Nexus of climate-smart agricultural technologies. Climate Services, 33, Article 100430. https://doi.org/10.1016/j.cliser.2023.100430

Deppisch, S., & Yilmaz, M. C. (2021). The impacts of urbanization processes on human rights. Current Urban Studies, 9(3), 355–375. https://doi.org/10.4236/cus.2021.93022

Eck, M. A., Murray, A. R., Ward, A. R., & Konrad, C. E. (2020). Influence of growing season temperature and precipitation anomalies on crop yield in the southeastern United States. Agricultural and Forest Meteorology, 291, Article 108053. https://doi.org/10.1016/j.agrformet.2020.108053

Enoguanbhor, E. C., Gollnow, F., Walker, B. B., Nielsen, J. Ø., & Lakes, T. (2021). Key challenges for land use planning and its environmental assessments in the Abuja city-region, Nigeria. Land, 10(5), Article 443. https://doi.org/10.3390/land10050443

Enoguanbhor, E. C., Gollnow, F., Walker, B. B., Nielsen, J. O., & Lakes, T. (2022). Simulating urban land expansion in the context of land use planning in the Abuja City-Region, Nigeria. GeoJournal, 87, 1479–1497. https://doi.org/10.1007/s10708-020-10317-x

Estrada, F., Botzen, W. J. W., & Tol, R. S. J. (2017). A global economic assessment of city policies to reduce climate change impacts. Nature Climate Change, 7(6), 403–406. https://doi.org/10.1038/nclimate3301

Franzke, C., Barbosa, S., Blender, R., Fredriksen, H., Laepple, T., Lambert, F., Nilsen, T., Rypdal, K., ... Yuan, N. (2020). The structure of climate variability across scales. Reviews of Geophysics, 58(2), Article e2019RG000657. https://doi.org/10.1029/2019RG000657

Gashure, S. (2025). Impacts of climate variability and adaptation strategies on staple crop productivity in Sidama, Ethiopia. Scientific Reports, 15, Article 27461. https://doi.org/10.1038/s41598-025-11880-4

Haysom, G., & Battersby, J. (2023). Urban food security and resilience. In C. Béné & S. Devereux (Eds.), Resilience and food security in a food systems context (pp. 355–388). Palgrave Macmillan. https://doi.org/10.1007/978-3-031-23535-1_11

Hu, G., Li, X., Liu, X., Wang, S., Zhang, X., Shi, X., Bai, X., & Hubacek, K. (2025). Mitigating the ripple effects of urbanisation on farmland productivity and ecological security through inclusive urbanisation strategies. npj Urban Sustainability, 5, Article 12. https://doi.org/10.1038/s42949-025-00199-8

Huang, Q., Liu, Z., He, C., Gou, S., Bai, Y., Wang, Y., & Shen, M. (2020). The occupation of cropland by global urban expansion from 1992 to 2016 and its implications. Environmental Research Letters, 15(8), Article 084037. https://doi.org/10.1088/1748-9326/ab858c

Ibe, E., Aliegba, E., & Umar, S. (2023). Implementation of urban policy and Sustainable Development Goal 11 in Federal Capital Territory (FCT), Abuja. African Journal of Political and Administrative Studies, 16(2). https://doi.org/10.4314/ajpas.v16i2.10

Ibilewa, D., Ishaya, S. K., & Magaji, J. I. (2021). Assessment of croplands' exposure to climate variability in the Federal Capital Territory (FCT), Abuja, Nigeria. International Journal of Environment and Climate Change, 11(1), 53–77. https://doi.org/10.9734/ijecc/2021/v11i130340

Idowu, D., & Zhou, W. (2021). Land use and land cover change assessment in the context of flood hazard in Lagos State, Nigeria. Water, 13(8), Article 1105. https://doi.org/10.3390/w13081105

Igbokwe, E. C., Musa, S., Anienwe, K., Oliha, A. O., & Anyadiegwu, P. C. (2024). A GIS-based approach for assessing urban development potential in Federal Capital Territory Nigeria. Asian Journal of Geographical Research, 7(3), 94–114. https://doi.org/10.9734/ajgr/2024/v7i3244

Imhanfidon, O. J., Bello, I. E., Mustapha, A., Odiji, C., Ihenacho, N. M., Tah, S. D., Modie, S., Nnaedozie, N., Moses, A., Afogbon, E., & Hellen, O. O. (2023). Geospatial assessment of the physical expansion in urban development in Bwari Area Council, Federal Capital Territory, Abuja. Advances in Social Sciences and Management, 1(10), 8–29. https://hspublishing.org/ASSM/article/view/201

Kemper, T., Melchiorri, M., Pesaresi, M., & Siragusa, A. (2016). Atlas of the human planet 2016: Mapping human presence on Earth with the Global Human Settlement Layer (Report No. EUR 28116 EN). European Commission, Joint Research Centre. https://doi.org/10.2788/889483

Mansour, S., Al-Belushi, M., & Al-Awadhi, T. (2020). Monitoring land use and land cover changes in the mountainous cities of Oman using GIS and CA-Markov modelling techniques. Land Use Policy, 91, Article 104414. https://doi.org/10.1016/j.landusepol.2019.104414

Melchiorri, M., Florczyk, A., Freire, S., Schiavina, M., Pesaresi, M., & Kemper, T. (2018). Unveiling 25 years of planetary urbanisation with remote sensing: Perspectives from the Global Human Settlement Layer. Remote Sensing, 10(5), Article 768. https://doi.org/10.3390/rs10050768

Meng, F., Reb, Z., Zang, P., Wang, C., Hong, S., Geng, R., Hong, W., Huang, B., ... Bai, Y. (2025). Estimation of the relationship between urban landscape pattern and crop yield by remote sensing data and field measurement. Remote Sensing, 17(22), Article 3667. https://doi.org/10.3390/rs17223667

Mshelia, Y. S., Onywere, S. M., & Letema, S. (2024). Modeling the spatial dynamics of land cover transitions and vegetation conditions in Abuja city, Nigeria. Urbanisation, Sustainability and Society, 1(1), 115–132. https://doi.org/10.1108/USS-12-2023-0026

Mubenga-Tshitaka, J. L., Dikgang, J., Muteba Mwamba, J. W., & Gelo, D. (2023). Climate variability impacts on agricultural output in East Africa. Cogent Economics & Finance, 11(1), Article 2181281. https://doi.org/10.1080/23322039.2023.2181281

Muhammad, F. S., Awudu, A., & Gazali, I. (2021). Adaptation implications of climate-smart agriculture in rural Pakistan. Sustainability, 13(21), Article 11702. https://doi.org/10.3390/su132111702

Ningi, T., Mphahlele, M., Sithole, V., Manyike, J. Z., Manganyi, B., Ngarava, S., Lubinga, M. H., Dladla, L., & Molepo, S. (2025). Assessment of the long-term impact of climate variability on food production systems in South Africa (1976–2020). Climate, 13(1), Article 8. https://doi.org/10.3390/cli13010008

Okeleye, S. O., Okhimamhe, A. A., Sanfo, S., & Fürst, C. (2023). Impacts of land use and land cover changes on migration and food security of North Central Region, Nigeria. Land, 12(5), Article 1012. https://doi.org/10.3390/land12051012

Rawat, J., & Kumar, M. (2015). Monitoring land use/cover change using remote sensing and GIS techniques: A case study of Hawalbagh block, district Almora, Uttarakhand, India. The Egyptian Journal of Remote Sensing and Space Science, 18(1), 77–84. https://doi.org/10.1016/j.ejrs.2015.02.002

Rowland, A., & Ebuka, A. O. (2024). Assessing the impact of land cover and land use change on urban infrastructure resilience in Abuja, Nigeria: A case study from 2017 to 2022. Structure and Environment, 16(1), 6–17. https://doi.org/10.30540/sae-2024-002

Rwanga, S. S., & Ndambuki, J. M. (2017). Accuracy assessment of land use/land cover classification using remote sensing and GIS. International Journal of Geosciences, 8(4), 611–622. https://doi.org/10.4236/ijg.2017.84033

Sang, L., Zhang, C., Yang, J., Zhu, D., & Yun, W. (2011). Simulation of land use spatial pattern of towns and villages based on CA–Markov model. Mathematical and Computer Modelling, 54(3–4), 938–943. https://doi.org/10.1016/j.mcm.2010.11.019

Schneider, A., & Woodcock, C. E. (2008). Compact, dispersed, fragmented, extensive? A comparison of urban growth in twenty-five global cities using remotely sensed data, pattern metrics and census information. Urban Studies, 45(3), 659–692. https://doi.org/10.1177/0042098007087340

Serote, B., Mokgehle, S., Senyolo, G., du Plooy, C., Hlophe-Ginindza, S., Mpandeli, S., Nhamo, L., & Araya, H. (2023). Exploring the barriers to the adoption of climate-smart irrigation technologies for sustainable crop productivity by smallholder farmers: Evidence from South Africa. Agriculture, 13(2), Article 246. https://doi.org/10.3390/agriculture13020246

Sheng, S., & Huang, J. (2025). Urban expansion and the loss of potential crop yield in the North China Plain: Implications for regional food security (1980–2020). Frontiers in Sustainable Food Systems, 9, Article 1545907. https://doi.org/10.3389/fsufs.2025.1545907

Tahir, Z., Haseeb, M., Mahmood, S. A., Batool, S., Abdullah-Al-Wadud, M., Ullah, S., & Tariq, A. (2025). Predicting land use and land cover changes for sustainable land management using CA-Markov modelling and GIS techniques. Scientific Reports, 15, Article 3271. https://doi.org/10.1038/s41598-025-87796-w

United Nations Department of Economic and Social Affairs. (2024). World population prospects 2024: Summary of results (Report No. UN DESA/POP/2024/TR/NO. 9). United Nations. https://population.un.org/wpp/assets/Files/WPP2024_Summary-of-Results.pdf

Wang, W., Wu, T., Li, Y., Xie, S., Han, B., Zheng, H., & Ouyang, Z. (2020). Urbanisation impacts on natural habitat and ecosystem services in the Guangdong-Hong Kong-Macao "Megacity." Sustainability, 12(16), Article 6675. https://doi.org/10.3390/su12166675

Wudil, A. H., Ali, A., Aderinoye-Abdulwahab, S., Raza, H. A., Mehmood, H. Z., & Sannoh, A. B. (2023). Determinants of food security in Nigeria: Empirical evidence from beneficiaries and non-beneficiaries rice farmers of the Kano River Irrigation Project. Frontiers in Sustainable Food Systems, 7, Article 999932. https://doi.org/10.3389/fsufs.2023.999932

Yiran, G., Ablo, A. D., Asem, F. E., & Owusu, G. (2020). Urban sprawl in sub-Saharan Africa: A review of the literature in selected countries. Ghana Journal of Geography, 12(1), 1–28. https://doi.org/10.4314/GJG.V12I1.1